

# FIBRE WAVINESS INDUCED BENDING IN COMPRESSION TESTS OF UNIDIRECTIONAL NCF COMPOSITES

Dennis Wilhelmsson<sup>1</sup>, Leif E. Asp<sup>1</sup>, Renaud Gutkin<sup>2</sup>, Fredrik Edgren<sup>3</sup>

<sup>1</sup>Chalmers University of Technology, Dept. Industrial and Materials Science, SE-41296 Gothenburg, Sweden

<sup>2</sup>Durability CAE Body & Trim, Volvo Car Corporation, 405 31 Gothenburg, Sweden

<sup>3</sup>GKN Aerospace Sweden AB, Flygmotorvägen, SE-46181 Trollhättan, Sweden

**Keywords:** Compression tests, NCF, Waviness, Bending

## ABSTRACT

Compression testing of carbon fibre composites according to ASTM D6641/D3410 is limited by a maximum of 10% bending for a valid test. This allowable was exceeded in a preceding study, where all the laminates had a large out-of-plane waviness. The aim of this study is to quantify the contribution from the out-of-plane fibre waviness to bending.

The fibre waviness was characterized on samples with high magnitudes of bending and the corresponding fibre misalignment angles were then mapped to a plane strain finite element model. This model represents the geometry through the thickness and in longitudinal direction. Virtual strain measurements and associated bending calculations could then be performed in Matlab from the strain field on the upper and lower surfaces, which resulted from compression loading. Virtual bending calculations have also been performed from strain measurements with an optical system (DIC).

The numerical model confirms that the out-of-plane waviness has an effect on bending. The magnitudes are however lower than expected, and lower than the experimental values. Bending was in the order of 5 % with a strain gauge of 5 mm, which constitutes half of the allowed amount of bending. It was also confirmed that the length of the strain gauge has a significant effect on the measured bending and on the experimental error.

## 1 INTRODUCTION

Experimental material characterization of carbon fibre reinforced polymers is both time consuming and costly. It is therefore very important to obtain as many valid tests from a campaign as possible. Compression tests according to ASTM D6641/D3410 [1,2] allows a maximum of 10% bending for a test to be considered valid, where bending is calculated from back-to-back strain measurements ( $\varepsilon_0$  and  $\varepsilon_1$ ) as

$$\frac{\varepsilon_0 - \varepsilon_1}{\varepsilon_0 + \varepsilon_1} \quad (1)$$

While conducting longitudinal compression tests of NCF composites, it was observed that many of the performed tests exceeded this allowable and the immediate question is whether these tests can be regarded as valid or not? This is the main motivation of the presented study.

It has already been established that the resulting local strain-field on the surface of a textile composite is inhomogeneous because of the heterogeneous material structure on the microscale [3]. One consequence is that the measured macroscopic strain will be incorrectly estimated if too small strain gages are used as they record an averaged local measure of strain [4]. But no explanation has yet been given on the underlying mechanism and how the microstructure affects bending in longitudinal compression tests.

By performing virtual strain measurements with a finite element (FE) model, we have been able to show how the fibre waviness of a unidirectional non-crimp fabric (NCF) composite cause an inhomogeneous strain field on the surface. But most importantly, an explanation can be given to how

the microstructure and the strain measurements affects the calculated bending in compression tests.

## 2 METHOD

### 2.1 Compression tests and specimens

All experimental results come from the study by Wilhelmsson et al. [5], where 12 unidirectional NCF laminates were tested in longitudinal compression according to ASTM D6641/D3410 [1,2]. These laminates were manufactured by resin transfer moulding (RTM) and contained different magnitudes of out-of-plane fibre waviness. Two laminates with high out-of-plane waviness were selected for this study, one with an average bending of 44 % (B2) and one with an average bending of 15 % (B3). See Table 1 for further details. All of the tested specimens were subjected to back-to-back strain measurements, which means that a 5 mm long strain-gauge was attached to each face.

Laminate	$n$	Layup	$t$ [mm]	$V_f$ [%]	$\bar{\theta}$ [°]	$\theta_{\max}$ [°]	ASTM D3410 / 6641	$\bar{B}_f$ [%]
B2	7	[0] <sub>10</sub>	2.03	53	2.8	8.0	1/6	44
B3	6	[0] <sub>11</sub>	2.03	59	2.6	8.2	1/5	15

Table 1: Information of the studied laminates, where  $n$  is the number of valid tests (all with strain-gauges),  $t$  is the thickness,  $V_f$  is the fibre volume fraction,  $\bar{\theta}$  is the mean fibre misalignment angle out-of-plane,  $\theta_{\max}$  is the maximum fibre misalignment angle out-of-plane and  $\bar{B}_f$  is the average bending for all the specimens of a laminate at failure.

### 2.2 Characterization of fibre waviness

The fibre waviness has been characterized with the method proposed by Wilhelmsson and Asp [6], where the angle of individual fibres is measured on high quality micrographs. An example of such a micrograph is presented in Figure 1 for a length equal to the gauge section (12 mm), where the out-of-plane waviness is clearly visible. The measured fibre misalignment angles which constitutes the fibre waviness are presented in Figure 2, where each cell has a size of 0.11x0.11 mm. The presented test specimen ‘B2-1’ is used throughout the method description and is also used in some representative plots in the result section.



Figure 1: Micrograph of a section in test specimen B2-1, which reveals the fibre waviness out-of-plane. The black regions are weft yarns in the NCF.

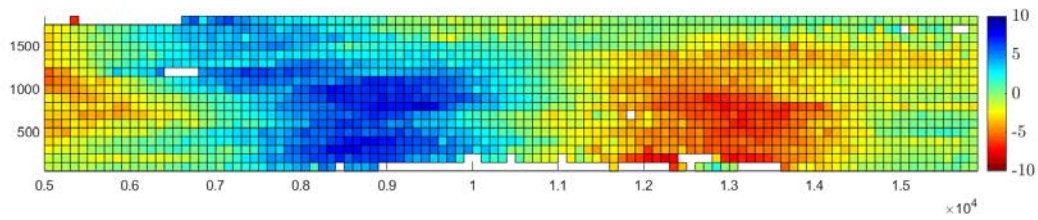


Figure 2: Fill plot of fibre misalignment angles with respect to a horizontal reference for specimen B2-1. A negative angle is defined as clockwise.

### 2.3 Finite element model

The experimentally characterized fibre misalignment angles are mapped to a finite element mesh in Abaqus as material orientations with a corresponding element size (0.11x0.11 mm). An example is shown in Figure 3 for specimen ‘B2-1’ where the principal orientations are presented as triads with a reduced symbol density. Elements of second order with reduced integration (CPE8R) are used under the assumption of plane strain conditions. The left boundary is coupled with multi-point-constraints to a reference node which is fixed in all degrees of freedom. The right boundary has similar couplings and restraints but a translation is prescribed in the longitudinal direction. The magnitude of this deformation is equivalent to the compressive failure strain of the laminate. Large deformation theory is considered in the analysis step. Material data are presented in Table 2 which are obtained from the study by Bru et al. [7] on the same material system.

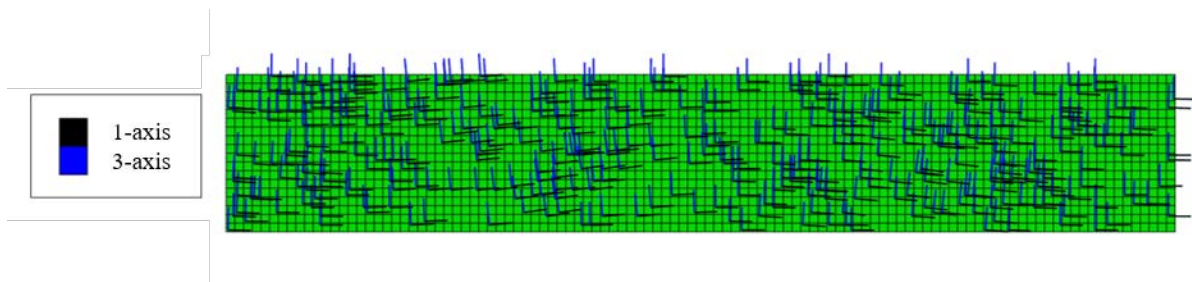


Figure 3: Material orientations in the FE model describing the out-of-plane fibre misalignments for specimen B2-1. The 1-direction is representing the fibre orientation.

$E_{11}$ [GPa]	$E_{33}$ [GPa]	$\nu_{12}, \nu_{13}$	$G_{13}$ [GPa]
132	9.3	0.28	4.4

Table 2: Elastic material properties used in the FE model. Direction 11 is in the fibre direction and 33 is the transverse direction to the fibres in the FE model.

### 2.4 DIC measurements

Optical strain measurements using digital image correlation (DIC) has been performed on three specimens from the B-laminate in compressive loading. Measurements are done on both surfaces for a compressive load equivalent to 30 % of the ultimate compressive load. Image acquisition has been performed with a DIC camera GO5000M-USB from JAI using a single 50 mm lens. The software GOM Correlate has been used to analyse the images.

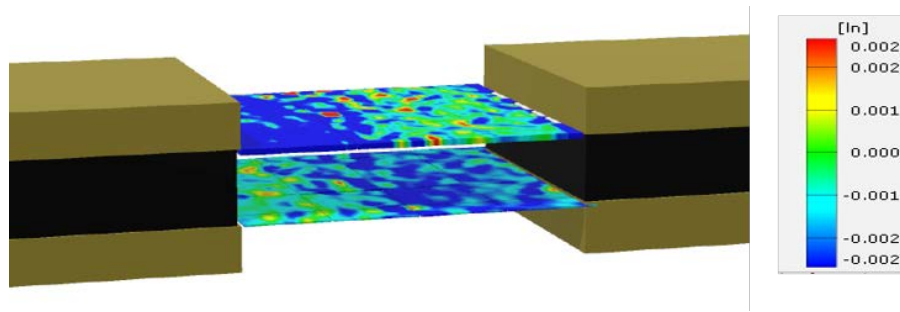


Figure 4: DIC results mapped to a 3D illustration of a test specimen and seen in an ISO view. The gauge section is made transparent to see the both the upper and lower surface in ISO view. Blue regions experience larger compressive longitudinal strains than green regions.

## 2.5 Virtual bending measurements

Recall the definition of bending according to ASTM [1,2] in equation 1. Virtual strain measurements are performed in Matlab by importing the longitudinal strain variation on the upper and lower surfaces from the FEM and DIC results. The experimental measurement strain from a conventional strain-gauge is a homogenised (average) value over its length. This is calculated in the virtual measurements as the mean over a predefined strain-gauge length. The measured bending is considered a random variable, which depends on the positions by which the physical strain-gauges are mounted in the experiment. A great advantage with the virtual bending calculations is that all possible positions of the strain-gauges can easily be evaluated. This is considered in the numerical assessment by performing strain measurements in all possible combinations of longitudinal positions of two virtual strain-gauges. The outcome is reported as a mean, maximum and standard deviation of bending. Bending is also calculated with a virtual strain-gauge length of 12 mm, which corresponds to a 100 % coverage of the surface.

## 3 RESULTS AND DISCUSSION

### 3.1 FE results

The test specimens have a large fibre waviness out-of-plane, which is caused mainly by the textile architecture and the manufacturing process. The weft yarns have not been explicitly modelled but rather the waviness caused by their extensions in the thickness and longitudinal direction. The plane strain model leans on the assumption of plane strain conditions and a constant geometry in the width direction of the specimens. This is an assumption since the weft yarns are threaded under and over each fibre bundle in the width direction of the specimen. Optical strain measurements using digital image correlation (DIC) were performed on both surfaces during compressive loading to validate this assumption. As can be seen from Figure 4, the strain field is almost constant across the width, which indicates that a 2D model is representative. The strain distributions along three paths have been extracted to quantitatively confirm this and these results are further discussed in section 3.2

As can be seen from the contour plot in Figure 5, the fibre waviness causes the longitudinal strain for specimen B2-1 to become inhomogeneous. The variation of longitudinal strain on the upper and lower surfaces is presented in Figure 6 for two samples from each laminate. The inhomogeneous strain field on the surfaces, which is discussed by Sánchez-Heres et al. [4] can clearly be seen from these plots. One explanation to these fluctuations can also be given here, namely the fibre waviness. The fluctuations seem to occur both on the mm and sub-mm length-scale. If specimen B-1 is considered, it can be seen that macroscopic bending occurs in the FE model in Figure 5, which agrees with the waviness profile in Figure 1. A similar type of macroscopic bending can be observed by the optical strain measurements in Figure 4 of specimen B2-10.

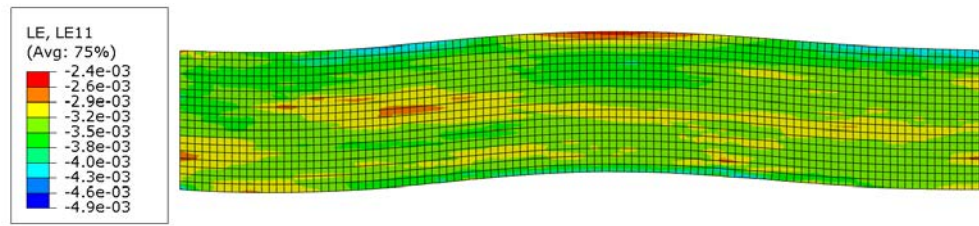


Figure 5: Contour plot of strains for specimen B2-1 loaded in longitudinal compression (x10 deformation scale). The average strain is equal to the compressive failure strain of 0.39 %.

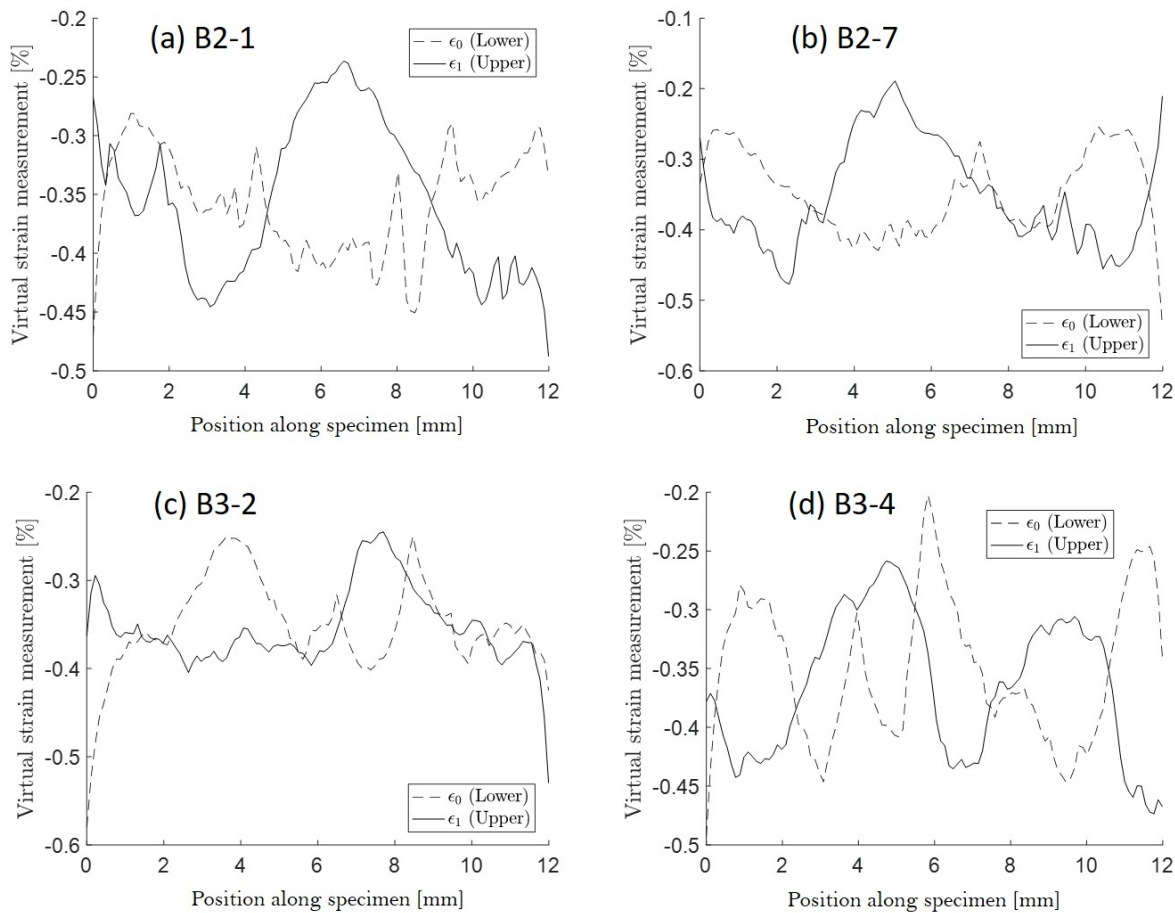


Figure 6: Longitudinal strain for specimens B2-1, B2-7, B3-2 and B3-4 along the upper and lower surfaces from the FE model (paths in the 2D model).

The longitudinal strain variations on the upper and lower surfaces in the numerical model are used to calculate bending according to ASTM [1,2] with the procedure described in section 2.4. Four specimens from each laminate have been studied and the outcome is presented in Table 3. The numerical model predicts higher bending for B2 than for B3, which agrees with the experimental data. The numerical predictions are however considerably smaller than the experimental values. The experimental values for bending is 44 % and 15 % whereas the numerical predictions are 6 % and 3 % respectively. It either means that the FE model is incapable of capturing the relevant mechanisms or that fibre waviness is not the main contribution to bending in the experiments.

*Bending values related to the FE model*

Specimen	Bending with 5 mm long physical strain- gauges [%]	Mean bending [%]	Maximum bending [%]	Bending with 12 mm long virtual strain- gauges [%]
B2-1		5.7	13.6	0.2
B2-3		6.8	12.9	0.6
B2-7		6.8	15.1	0.4
B2-8		5.1	11.6	0.8
<b>B2 average</b>	<b>44</b>	<b>6.1</b>	<b>13.3</b>	<b>0.5</b>
B3-2		3.0	8.1	0.4
B3-4		1.8	5.1	2.0
B3-5		4.9	9.6	1.9
B3-9		2.5	5.9	1.8
<b>B3 average</b>	<b>15</b>	<b>3.1</b>	<b>7.2</b>	<b>1.5</b>

Table 3: Statistics of bending related to the FE model for four specimens from laminates B2 and B3. The average from calculations based on experimental values from strain gauges are also presented.

Sánchez-Heres et al. [4] concluded that increasing the gage size decreases the size of the strain measurement error, ultimately improving the accuracy of the characterization method. This can be confirmed by the results in Figure 7, where the strain-gauge size was altered between 2 and 12 mm in steps of 2mm. Both the average reported bending and the measurement error is decreased with an increased strain-gauge size. It is not feasible to attach 12 mm long strain-gauges to surface which has the same length but there is a significant improvement already for 8 mm long over 5 mm which has been used in the experimental study [5].

Experimental results of bending as a function of compressive strain show constant behavior after an initial peak value. This peak value may be caused by some sort of misalignment while clamping the specimen. The effect of this can be studied with the current FE model by prescribing a rotation in a preceding analysis step. Preliminary results show that this problem can be a large contributing factor to a high measured bending. An initial misalignment angle of only half a degree for one side of the specimen results in an increase in bending from 5.7 % to 27 % for specimen B2-1. It should be stated that the chosen rotation angle was such that it contributed to the bending caused by fibre waviness. Further studies are suggested on this topic to increase the understanding of sources to bending in compression tests.

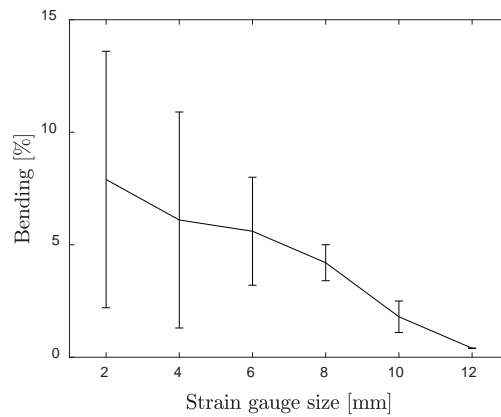


Figure 7: Bending as function of virtual strain-gauge length for specimen B2-1. The bending value is presented as the average from all possible placement combination with the associated standard deviation.

### 3.2 DIC results

Virtual bending calculations have been made on strain distributions from DIC images by the procedure presented in section 2.5. These results may be seen as complementary to the results obtained by the FE model since the isolated effect on bending from waviness cannot be studied.

Unfortunately, DIC measurements have not been performed on the same laminates for which the waviness has been characterized as input for the FE model. Instead, two other laminates from the study by Wilhelmsson et al. have been analysed [5].

The variation of longitudinal strain on the upper and lower surfaces is presented in Figure 7 for two samples from each laminate. Inhomogeneous strain fields on the surfaces can be observed, similar to those generated by the numerical model. Three specimens from each laminate have been studied in total and the bending calculations are presented in Table 4. These results confirm the high bending values obtained by physical strain gauges in the experimental tests.

The bending values for laminate B1, based on three different strain paths, show similar values and we argue that these values are representative of low variations across the width.

*Bending values related to the DIC measurements*

Specimen	Bending with 5 mm long physical strain-gauges [%]	Mean bending (L, C, R) [%]	Maximum bending (L, C, R) [%]	Bending with 12 mm long virtual strain-gauges (L, C, R) [%]
B1-8		32, 24, 22	58, 57, 56	3, 7, 5
B1-9		27, 33, 28	79, 82, 74	23, 22, 4
B1-10		25, 39, 32	63, 81, 67	15, 12, 8
<b>B1 average</b>	<b>61</b>	<b>29</b>	<b>69</b>	<b>11</b>
C1-1		18	57	10
C1-11		21	43	12
C1-26		38	56	33
<b>C1 average</b>	<b>19</b>	<b>26</b>	<b>52</b>	<b>18</b>

Table 4: Statistics of bending related to the DIC measurements for three specimens from laminates B1 and C1. L, C and R represents strains extracted along a line from the left, center or right region of the surface. The average from calculations based on experimental values from physical strain gauges are also presented.

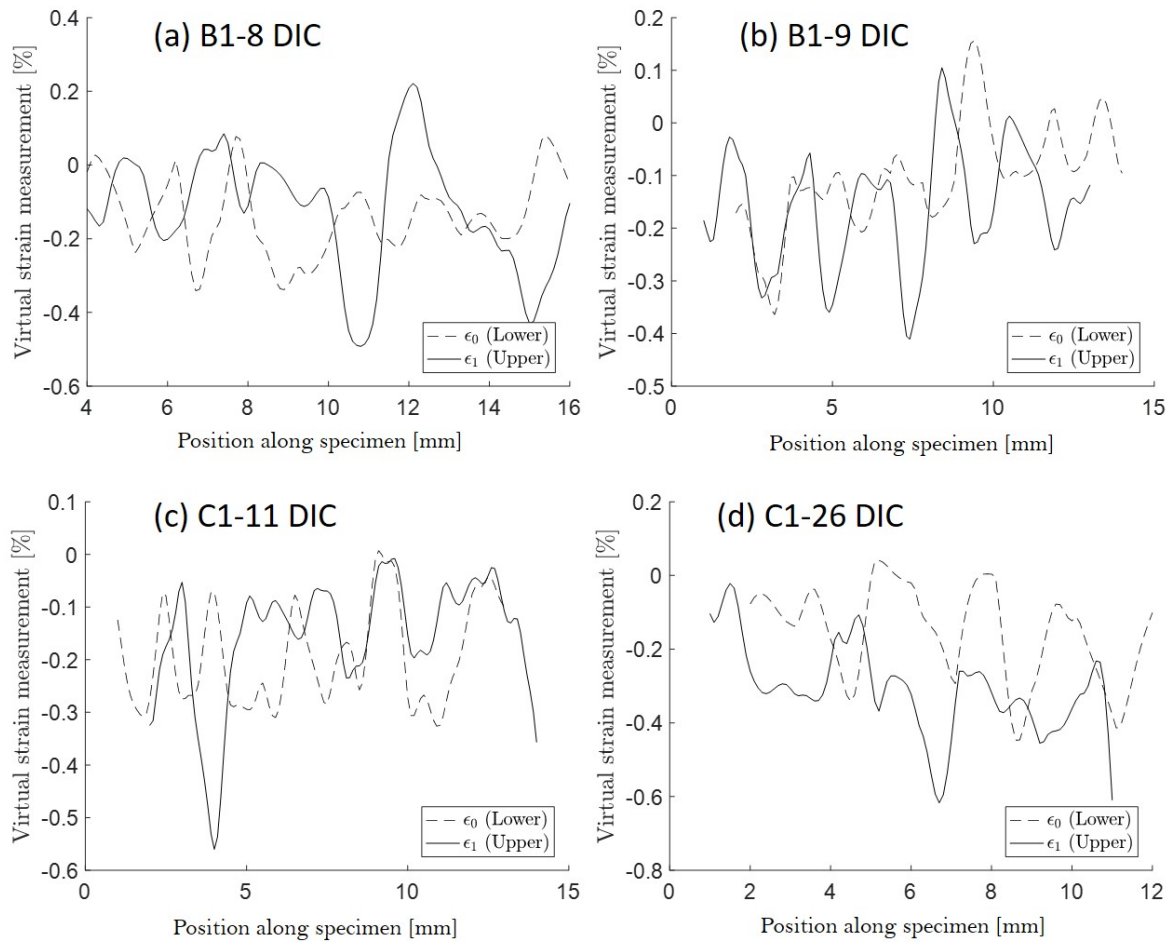


Figure 8: Longitudinal strain for specimens B1-8, B1-9, C1-11 and C1-26 along paths on the upper and lower surfaces from the DIC measurements.

#### 4 CONCLUSIONS

Unidirectional NCF composites with large out-of-plane waviness were tested in compression in a preceding study, where the measured bending exceeded the allowed value according ASTM [1,2]. The hypothesis was that the waviness is contributing to the measured bending. An FE model has been developed, which is based on the experimentally characterized fibre misalignment angles from the compression study by Wilhelmsson et al. [5]. This model has then been used to perform virtual bending measurements.

Virtual bending measurements have also been performed on strain data obtained by DIC. Firstly, these results confirm the high bending values obtained by physical strain gauges. Secondly, a relatively low effect on bending could be shown for three different positions in the width direction, which validates the use of a 2D model. And thirdly, measurements from the DIC images shows an inhomogeneity, which is similar to the strain plots from the FE model.

Four test specimens from two laminates have been studied with the FE model and the conclusion is that the mode can predict a difference in bending between these, which agrees with the experimental observations. The bending mode does also agree with the shape of the waviness as expected. The model does however show that the effect of out-of-plane waviness on bending is lower than expected. The FE model predicts a bending of 3 % and 6 % whereas that experimental measurements show 15 % and 44 %.

It has been established in a previous study that the strain field on the surface of an NCF composite is



inhomogeneous and that the strain measurement technique must be considered to maintain accuracy [4]. This study gives a physical motivation to why the inhomogeneous strain field occurs on the surface, namely the out-of-plane fibre waviness.

The effect of size of the strain-gauges have been studied and may be used as a guideline for compression testing of laminates with high out-of-plane waviness. The main conclusion is the same as in previous studies [3,4], namely that a sufficient size of the strain-gauges in the longitudinal direction must be used. DIC measurements does however show that the effect on bending of the strain-gauge width should be less sensitive.

As a final remark, it can be concluded from our combined numerical and experimental study, that the measured bending due to high out-of-plane waviness is in the order of 5 % with a strain gauge of 5 mm. This constitutes half of the allowed amount of bending according to ASTM [1,2], which is 10 %.

### ACKNOWLEDGEMENTS

This work has been performed within the Swedish Aeronautical Research Program (NFFP), Project 2013-01119, jointly funded by the Swedish Armed Forces, Swedish Defence Materiel Administration, the Swedish Governmental Agency for Innovation Systems and GKN Aerospace. Sweden's innovation agency, VINNOVA, are gratefully acknowledged for funding via LIGHTer SRA1. Peter Hällström and Thomas Bru performed major parts of the DIC measurements at Swerea Sicomp. Their work is gratefully acknowledged.

### REFERENCES

- [1] ASTM. ASTM D3410 - Standard Test Method for Compressive Properties of Polymer Matrix Composite Materials with Unsupported Gage Section by Shear. vol. 3. 2008. doi:10.1520/D3410.
- [2] ASTM. ASTM D6641 - Standard Test Method for Compressive Properties of Polymer Matrix Composite Materials Using a Combined Loading Compression ( CLC ) Test Fixture. vol. i. 2014. doi:10.1520/D6641.
- [3] Lang EJ, Chou T-W. The effect of strain gage size on measurement errors in textile composite materials. *Compos Sci Technol* 1998;58:539–48. doi:10.1016/S0266-3538(97)00166-8.
- [4] Sánchez-Heres LF, Ringsberg JW, Johnson E. Characterization of Non-Crimp Fabric Laminates: Loss of Accuracy Due to Strain Measuring Techniques. *J Test Eval* 2016;44:20150051. doi:10.1520/JTE20150051.
- [5] Wilhelmsson D, Asp LE, Gutkin R, Edgren F. An experimental study of fibre waviness and its effects on compressive properties in unidirectional NCF composites. To Be Submitted 2017.
- [6] Wilhelmsson D, Asp LE. A direct method for characterization of fibre misalignment angles in composites. To Be Submitted 2017.
- [7] Bru T, Hellström P, Gutkin R, Ramantani D, Peterson G. Characterisation of the mechanical and fracture properties of a uni-weave carbon fibre/epoxy non-crimp fabric composite. *Data Br* 2016;6:680–95. doi:10.1016/j.dib.2016.01.010.